High-Efficiency Spiral Zone Plates in Sapphire

Yi-Ming Lu, Zhen-Nan Tian, Shuang-Ning Yang, Jian-Guan Hua, Xue-Qing Liu, Yang Zhao, Qi-Dai Chen, Yong-Lai Zhang, and Hong-Bo Sun, *Fellow, IEEE*

***Abstract*— Here, we report embedded spiral zone plates (SZPs) processed by tightly focused femtosecond pulses, inducing a refractive index change in a sapphire crystal. The change in the index is investigated both experimentally and theoretically and found to be 0.93% lower than that before the laser irradiation. Benefiting from the investigation of the photorefraction, a high diffractive efficiency of up to 78% is achieved for the SZPs. In addition, the SZPs are embedded under the surface of the sapphire, which ensures that the components possess stable optical properties in the case of external refractive index changes. The high-performance elements having a high diffractive efficiency and stable optical performance will have tremendous applications in optical communication and optical manipulation.**

***Index Terms*— Femtosecond laser, sapphire, OV beam, spiral zone plates.**

I. Introduction

In the past decades, with the development of diffractive optics, diffractive micro-optical elements have received new relevance and new models have been developed for them, leading to a significant impact on the development of optical systems. Until now, they have been a key part of optical communication and interconnection applications and widely used in the aerospace and military fields. Simultaneously, the efficiency of diffractive optical elements (DOEs) has been undergoing an applicable revolution. Despite the long period of research, their low efficiency is still the toughest problem limiting the integration of diffractive optical micro-elements. To solve this issue, the conventional amplitude-type diffractive elements are replaced by phase-type devices [1]–[5] and the order of the corresponding diffractive devices is increased [3]–[5]. High-efficiency diffractive elements have been reported to be designed based on the total internal reflection [6], stratified volume diffraction [7], and polarization-modulating structures [8]. Recently, developing a meta-surface has become a concerned prominent area to improve the diffractive efficiency [9]–[11]. The above-mentioned works have played a crucial role in the research and development of high-efficiency DOEs.

The fabrication of continuous-surface elements to achieve improved diffractive efficiency is an easy operating and highly feasible method. Recently, there have been several reports on using laser direct writing lithography to fabricate continuous-surface micro-optical elements on hybrid sol-gel materials [12], [13]. Similarly, in a related letter, the fabrication of continuous-surface spiral zone plates (SZPs) on SU-8 by femtosecond (fs)-laser direct writing based on a two-photon polymerization was proposed [14]. It was the basis for a report from the Xie group on a single-focus SZP [15]. However, all the above-mentioned studies on SZP fabrication were focused on the surface of the relevant material, which was sensitive to the external changing environment, such as in a sea or desert. The fs-laser direct writing technology [16]–[19] is playing an essential role in embedded micro-optical components because the focused fs-laser can easily induce a change in the refractive index of the transparent material without causing any damage to the surface [20], [21]. Accordingly, numerous three-dimensional structures have been fabricated, such as chiral structures and integrated opto-mechanical single-photon frequency shifters.

Here, we present a continuous-surface SZP in a sapphire to generate a high-efficiency optical vortex (OV) beam by fs-laser direct writing. The high-precision fs-laser point-by-point scanning method provides the technical support for the fabrication of arbitrary three-dimensional volume structures in the transparent material. Serial pulses and same pulse energy ensure that the profile of the fabricated structure is a continuous surface. Thus, the high-efficiency DOEs in the sapphire exhibit an excellent optical performance and can be applied in optical communication, quantum calculation, and quantum information in the aerospace and military domains where the harsh environment demands that a material endures a high temperature and resists corrosion.

II. Theory and Experiments

In the experiment, a third-harmonic wavelength UV light (343 nm) is generated by a Pharos fs-laser amplifier (repetition $f = 200$ kHz and pulse duration $\tau_p = 280$ fs). A high-numerical aperture lens (NA = 0.75, magnification 40×) is used to tightly focus the laser on the $d = 1.22\lambda/NA = 558$ nm distance spots in a 430-μm-thick sapphire (He Fei Ke Jing Material Technology, Ltd). The precise scanning of the light in the xy plane is controlled by a two-Galvano-mirror system, and the sample is moved unrestrictedly along

Manuscript received April 17, 2019; accepted April 23, 2019. Date of publication April 29, 2019; date of current version June 3, 2019. This work was supported in part by the National Key R&D Program of China under Grant 2017YFB1104600 and in part by the National Natural Science Foundation of China (NSFC) under Grants #61590930, #61805098, #61825502 and #61435005.

Y.-M. Lu, Z.-N. Tian, S.-N. Yang, J.-G. Hua, Y. Zhao, Q.-D. Chen, and Y.-L. Zhang are with the State Key Laboratory of Integrated Optoelectronics, College of Electronic Science and Engineering, Jilin University, Changchun 130012, China (e-mail: zhennan_tian@jlu.edu.cn).

X.-Q. Liu and H.-B. Sun are with the State Key Laboratory of Precision Measurement Technology and Instruments, Department of Precision Instrument, Tsinghua University, Beijing 100084, China (e-mail: hbsun@tsinghua.edu.cn).

Color versions of one or more of the figures in this letter are available online at http://ieeexplore.ieee.org.

Digital Object Identifier 10.1109/LPT.2019.2913712

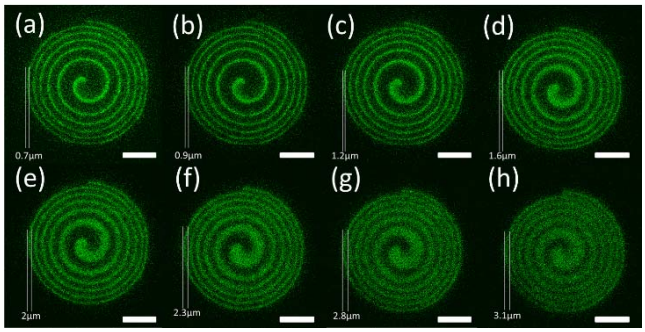

Fig. 1. (a)–(h) Fluorescence confocal microscope images of a particular structure fabricated by 280 fs, 343 nm wavelength, and 18 nJ (at focus) in the sapphire at different depths (0 μm, 10 μm, 20 μm, 30 μm,40 μm, 50 μm, 60 μm, and 68 μm). Scale bar: 15 μm.

the z axis by a piezo stage (PI P611 ZS, 1 nm precise). The scanning speed as controlled by a program is 40 μm/s. The high-repetition laser combined with high-speed scanning enables rapid fabrication of DOEs (several minutes). Based on the scanning speed and repetition frequency, the pulse-to-pulse spatial distance is calculated by $x = v_s/f$ to be 0.2 nm, which is beneficial for fabricating SZPs with smooth profiles in the sapphire [23]–[25]. Unless otherwise stated, in this study, the fabricating pulse energy is 18 nJ and layer spacing is 500 nm, which are the most appropriate parameters for fabricating continuous-surface elements without any cracks.

For general DOEs, such as two-level Fresnel zone plates, most of the light is scattered when it passes through them. This undesirable scattering not only causes light loss but also reduces the contrast of the image plane. Benefiting from the three-dimensional processing ability of the fs-laser, continuous-surface SZPs were processed inside the sapphire. An SZP of 60 μm in diameter and 68 μm in height was observed by 40× fluorescence confocal microscope at different depths, and the results are shown in Figs. 1(a)–1(h), respectively. In Fig. 1(a), the image is captured 40 μm below the surface. Then the microscope observation plane moves down gradually, and Figs. 1(b)–(h) show the images captured at intervals of 10 μm. The width of the helix at the edge of the SZP increases from 0.7 mm to 3.1 mm, which indicates that an SZP with a continuous surface is fabricated inside the sapphire by the high-precision fs-laser fabrication

III. Results and Discussion

It is well known that multi-photon ionization is the main cause of the optical breakdown occurring in dielectrics [26]. In this experiment, a nearly two-photon generation by the used 343-nm-wavelength laser is required to transfer an electron from the valence band to the conduction band. A crystal-amorphous-re-crystal transition can be easily achieved by laser-material interaction, which changes the refractive index of the transparent material. Thus, the difference in the refractive index between the laser-modified region of the sapphire and host sapphire can modulate the phase to achieve some distinct optical effects [27]. However, the refractive index change cannot be calculated accurately because it depends on the pulse energy, aperture of the objective lens, repetition, and material. Therefore, some SZPs of different heights need to be

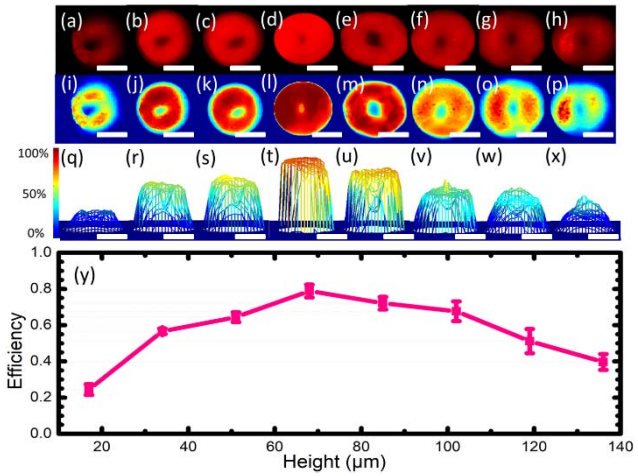

Fig. 2. Light spots (a)–(h), energy extraction diagrams (i)–(p), three-dimensional grid diagrams (q)–(x) on the focus plane generated by different-height SZPs, and the normalized spot energy obtained by the integration of the light spots (z). The peak in the efficiency curve (78%) occurs when the height is 68 μm. Scale bar: 1 μm.

fabricated to form the highest-efficiency elements to calculate accurately the refractive changing index. In fact, the refractive index change varies with the depth. The refractive index is changed less because of defocusing when the same pulse laser focuses deeper inside a transparent material. Moreover, we assume that the refractive index changes of each laser-modified region are the same in the experiment. During the measurement, a He-Ne laser (Peking University Factory of the Physics Department) was used. The power of the laser incident on the SZP was 3 μw. The diffractive beam was captured by an imaging system composed of a 40× objective lens and an industrial CCD camera (5.0 Megapixels). To ensure the comparability of the different structural tests, the exposure, brightness, and contrast were set as −5, 141, and 43, respectively. The light spots on the focal plane of the SZPs of different heights (17 μm, 34 μm, 51μm, 68 μm, 85 μm, 102 μm, 119 μm, and 136 μm) are shown in Figs. 2(a)–(h). To display the focusing spots of the different height elements more directly and clearly, the energy extraction diagrams and three-dimensional grid diagrams of the original images are shown in Figs. 2(i)–(p) and Figs. 2(q)-(x), respectively. The normalized spot energy is obtained from the integration of the light spots. It is found that the normalized diffraction efficiency first increases and then decreases with the change in the component thickness, as shown in Fig. 2(y).

DOE with 68 μm height has the highest efficiency of 78%, and the refractive changing index is calculated by the equation,

$$\Delta\phi = 2\pi\,\Delta n h/\lambda \tag{1}$$

where h is the height of the SZP and λ is the measured laser wavelength. For DOEs, working at the maximum efficiency, the phase delay varies continuously from 0 to 2π. A refractive changing index of 9.31×10^{-3} is obtained by formula (1), which agrees well with the previous reports on the fs-laser direct writing process applied to a sapphire at the threshold value [28].

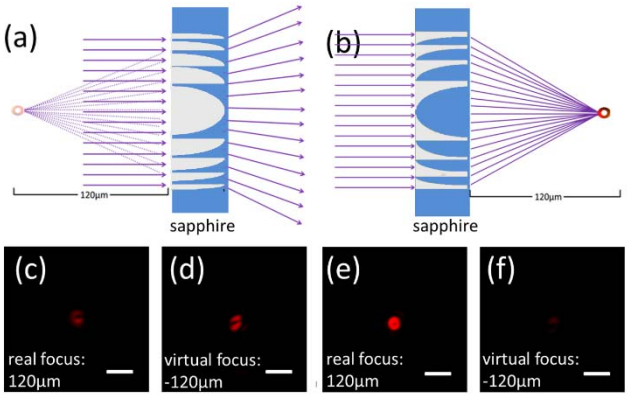

Fig. 3. Two different SZPs modeled by a concave lens (a) and convex lens (b). The diffractive focus of the SZP designed as a concave lens (positive refractive index change) at the real focus (c) and virtual focus (d). The diffractive focus of the conjugate structure designed as a convex lens (negative refractive index change) at the real focus (e) and virtual focus (f). Focus length: 120 μm and scale bar: 6 μm.

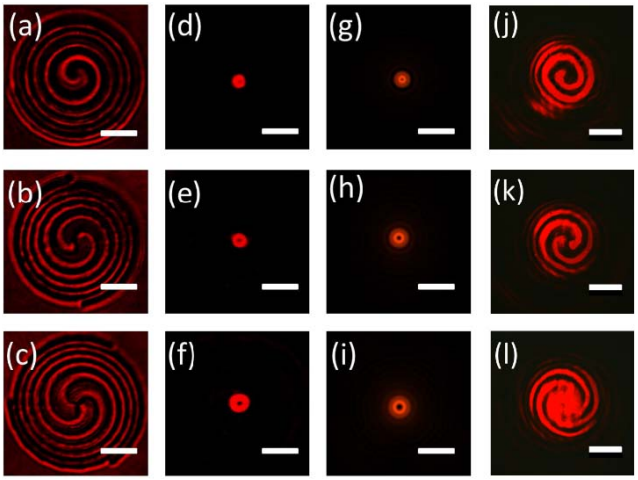

Fig. 4. SZPs with different topological charges of one, two, and three (a)–(c), experiment results (d)–(f), simulation results (g)-(i), and the interference patterns of the OAMs (j)–(l). Scale bar: 18 μm (a)-(c) and 6 μm (d)–(l).

Although the refractive changing index is calculated, the positive or negative of the amount of the fs-laser modified refractive changing index is not obtained. It is well established that when a laser exceeds the damage threshold, the high peak energy of the laser instantly transforms a crystal of sapphire into plasma to form a void. In the case when the laser power approaches the damage threshold, the peak power will form a photo-modified region having a decreased refractive index instead of a void. According to the law of conservation of mass, the surrounding host sapphire will then acquire a mass density because of the fs-laser-modified volume expansion [29], [30]. For the three-dimensional structures in the considered sapphire, the same method can be used for explaining that refractive index of the region induced by the fs-laser is smaller than that of the host sapphire. It is important to know the refractive index changes of the region induced by laser because the phase change value is related to it. The diffractive efficiency of an optical element depends on its refractive index distribution and the refractive index of its surrounding environment. To provide the evidence for the increasing or decreasing refractive index of the fs-laser-scanning region directly, Two SZPs modeled by a concave lens and convex lens were fabricated, respectively. The scanned area and unscanned area are marked in gray and blue in Figs. 3(a) and 3(b), respectively. If the refractive index increases, a donut shaped focus is formed behind the SZP (Fig. 3(a)), having a higher energy than that in its front. However, the focus energy in front of the SZP (Fig. 3(d)) is obviously higher than that in the back (Fig. 3(c)). It can be observed that the refractive index of the laser scanning region is reduced. As for the conjugate structure, the element, as shown in Fig. 3(b), possesses a brighter spot behind the element (Fig. 3(e)) than the one in front (Fig. 3(f)). This indicates that the refractive index of the laser scanning region is decreased, and the element is seen as consisting of unscanned blue areas.

The OV beam has a circular ring cross-section intensity distribution, a spiral wave-front phase distribution, and an orbital angular momentum. Compared with a general light wave, the OV beam possesses a hollow spot on the focusing plane, instead of a solid spot [31]. The theoretical and experimental spot sizes of the SZPs with different topological charges are shown in Fig. 4. Three SZPs are fabricated with different topological charges of one, two, and three, as shown in Figs. 4(a)–(c). When the He-Ne laser passes through the element, a hollow spot appears at the focus. The experiment light spots (Figs. 4(d)–(f)) are in good agreement with the theoretical results (Figs. 4(g)–(i)) simulated by the commercial optical software, Virtual Lab. In addition, the interference patterns of the OAM beams with different topological charges and plane wave are shown in Figs. 4(j)–(l).

IV. Conclusions

Overall, a three-dimensional continuous optical element can be achieved inside a transparent material by laser-induced refractive index changes. A high-efficiency SZP was fabricated in a sapphire by femtosecond-laser direct writing intensive scanning. A high diffractive efficiency (78%) of the SZP was measured accurately via the gray-scale integral method. Simultaneously, perfect and homogeneous OV beams focused on the SZPs with topological charge numbers of one, two, and three were obtained. We also verified that the refractive index of the sapphire exposed by the femtosecond laser was reduced theoretically and experimentally, and the refractive changing index (Δn) was 9.31×10^{-3}. The SZP elements embedded in the sapphire possessed the excellent property of being insensitive to the changes in the external refractive index and exhibited a tremendous potential for applications in harsh environments. The OAM offers unprecedented freedom to quantum communication and shows tangible prospects in the field of optical manipulation.

References

[1] C. Wang *et al.*, "Phase-type quantum-dot-array diffraction grating," *Rev. Sci. Instrum.*, vol. 79, no. 12, Dec. 2008, Art. no. 123502.

[2] P. Srisungsitthisunti, O. K. Ersoy, and X. Xu, "Volume Fresnel zone plates fabricated by femtosecond laser direct writing," *Appl. Phys. Lett.*, vol. 90, no. 1, Jan. 2007, Art. no. 011104.

[3] E. D. Fabrizio *et al.*, "High-efficiency multilevel zone plates for keV X-rays," *Nature*, vol. 401, no. 6756, pp. 895–898, Oct. 1999.

[4] K. Yamada, W. Watanabe, Y. Li, K. Itoh, and J. Nishii, "Multilevel phase-type diffractive lenses in silica glass induced by filamentation of femtosecond laser pulses," *Opt. Lett.*, vol. 29, no. 16, pp. 1846–1848, Aug. 2004.

[5] Y. L. Sun *et al.*, "Protein-based soft micro-optics fabricated by femtosecond laser direct writing," *Light Sci. Appl.*, vol. 3, p. e129, Oct. 2014.

[6] M. S. D. Smith and K. A. Mcgreer, "Diffraction gratings utilizing total internal reflection facets in Littrow configuration," *IEEE Photon. Technol. Lett.*, vol. 11, no. 1, pp. 84–86, Jan. 1999.

[7] R. Johnson and A. Tanguay, "Stratified volume holographic optical elements," *Opt. Lett.*, vol. 13, no. 3, pp. 189–191, Mar. 1988.

[8] H. Lajunen, J. Tervo, and J. Turunen, "High-efficiency broadband diffractive elements based on polarization gratings," *Opt. Lett.*, vol. 29, no. 8, pp. 803–805, Apr. 2004.

[9] S. Shrestha, A. C. Overvig, M. Lu, A. Stein, and N. Yu, "Broadband achromatic dielectric metalenses," *Light Sci. Appl.*, vol. 7, no. 1, p. 85, Nov. 2018.

[10] M. Papaioannou, E. Plum, E. T. Rogers, and N. I. Zheludev, "All-optical dynamic focusing of light via coherent absorption in a plasmonic metasurface," *Light Sci. Appl.*, vol. 7, no. 3, Mar. 2018, Art. no. e17157.

[11] S. Bajt *et al.*, "X-ray focusing with efficient high-NA multilayer Laue lenses," *Light Sci. Appl.*, vol. 7, no. 3, Mar. 2018, Art. no. e17162.

[12] W. X. Yu, X.-C. Yuan, N. Q. Ngo, W. X. Que, W. C. Cheong, and V. Koudriachov, "Single-step fabrication of continuous surface relief micro-optical elements in hybrid sol-gel glass by laser direct writing," *Opt. Express*, vol. 10, no. 10, pp. 443–448, May 2002.

[13] W. Cheong, X.-C. Yuan, V. Koudriachov, and W. X. Yu, "High sensitive SiO_2/TiO_2 hybrid sol-gel material for fabrication of 3 dimensional continuous surface relief diffractive optical elements by electron-beam lithography," *Opt. Express*, vol. 10, no. 14, pp. 586–590, Jul. 2002.

[14] Z. N. Tian *et al.*, "Mirror-rotation-symmetrical single-focus spiral zone plates," *Opt. Lett.*, vol. 43, no. 13, pp. 3116–3119, Jul. 2018.

[15] Y. Liang, E. Wang, Y. Hua, C. Q. Xie, and T. Ye, "Single-focus spiral zone plates," *Opt. Lett.*, vol. 42, no. 13, pp. 2663–2666, Jul. 2017.

[16] W. Wang *et al.*, "Direct laser writing of superhydrophobic PDMS elastomers for controllable manipulation via marangoni effect," *Adv. Funct. Mater.*, vol. 27, no. 44, Nov. 2017, Art. no. 1702946.

[17] L. Wang *et al.*, "Plasmonic nano-printing: Large-area nanoscale energy deposition for efficient surface texturing," *Light Sci. Appl.*, vol. 6, no. 12, Dec. 2017, Art. no. e17112.

[18] J. Yang *et al.*, "Design and fabrication of broadband ultralow reflectivity black Si surfaces by laser micro/nanoprocessing," *Light Sci. Appl.*, vol. 3, no. 7, Jul. 2014, Art. no. e185.

[19] X.-Q. Liu *et al.*, "Dry-etching-assisted femtosecond laser machining," *Laser Photon. Rev.*, vol. 11, no. 3, May 2017, Art. no. 1600115.

[20] F. Chen and J. V. de Aldana, "Optical waveguides in crystalline dielectric materials produced by femtosecond-laser micromachining," *Laser Photon. Rev.*, vol. 8, no. 2, pp. 251–275, Mar. 2014.

[21] H. Liu, C. Cheng, C. Romero, J. R. V. de Aldana, and F. Chen, "Graphene-based Y-branch laser in femtosecond laser written Nd: YAG waveguides," *Opt. Express*, vol. 23, no. 8, pp. 9730–9735, Apr. 2015.

[22] R. R. Gattass and E. Mazur, "Femtosecond laser micromachining in transparent materials," *Nature Photon.*, vol. 2, no. 4, pp. 219–225, Apr. 2008.

[23] K. Sugioka and Y. Cheng, "Ultrafast lasers–reliable tools for advanced materials processing," *Light Sci. Appl.*, vol. 3, no. 4, p. e149, Apr. 2014.

[24] L. Fan *et al.*, "Integrated optomechanical single-photon frequency shifter," *Nature Photon.*, vol. 10, no. 12, pp. 766–770, Dec. 2016.

[25] F. Flamini *et al.*, "Thermally reconfigurable quantum photonic circuits at telecom wavelength by femtosecond laser micromachining," *Light Sci. Appl.*, vol. 4, no. 11, p. e354, Nov. 2015.

[26] B. Poumellec, M. Lancry, R. Desmarchelier, E. Hervé, and B. Bourguignon, "Parity violation in chiral structure creation under femtosecond laser irradiation in silica glass," *Light Sci. Appl.*, vol. 5, no. 11, Nov. 2016, Art. no. e161780.

[27] J. Ni *et al.*, "Three-dimensional chiral microstructures fabricated by structured optical vortices in isotropic material," *Light Sci. Appl.*, vol. 6, Jul. 2017, Art. no. e17011.

[28] Q.-K. Li *et al.*, "Multilevel phase-type diffractive lens embedded in sapphire," *Opt. Lett.*, vol. 42, no. 19, pp. 3832–3835, Oct. 2017.

[29] S. Juodkazis *et al.*, "Laser-induced microexplosion confined in the bulk of a sapphire crystal: Evidence of multimegabar pressures," *Phys. Rev. Lett.*, vol. 96, no. 16, Apr. 2006, Art. no. 166101.

[30] S. Juodkazis *et al.*, "Control over the crystalline state of sapphire," *Adv. Mater.*, vol. 18, no. 11, pp. 1361–1364, Jun. 2006.

[31] L. Yang *et al.*, "Direct laser writing of complex microtubes using femtosecond vortex beams," *Appl. Phys. Lett.*, vol. 110, no. 22, May 2017, Art. no. 221103.